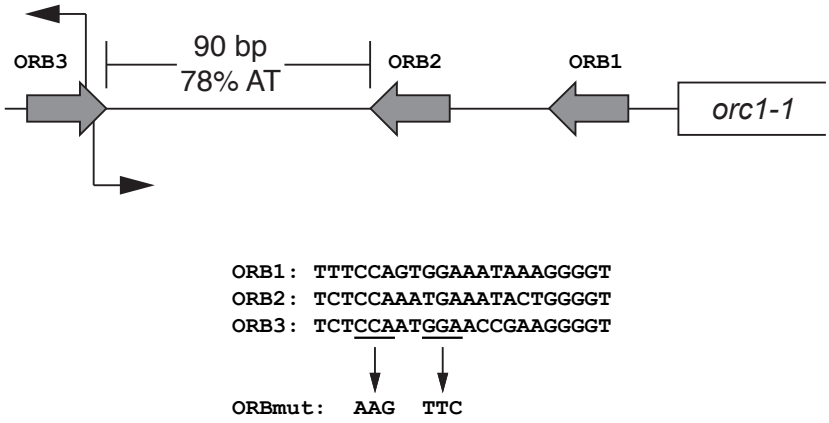

Figure S1. Related to Figure 1. Schematic of *oriC1.* Cartoon showing the three ORB elements of *oriC1* (grey arrows) and the *orc1-1* gene (open white box). Black arrows indicate where replication initiates *in vivo*. The consensus sequences for ORBs 1-3 are listed below. The six bases that were mutated in the ORB elements (see Fig. 1C) are underlined and black arrows point to the resulting sequence substitutions. Our previous work has revealed that these mutations abrogate interaction with Orc1-1 (Robinson et al., 2004).

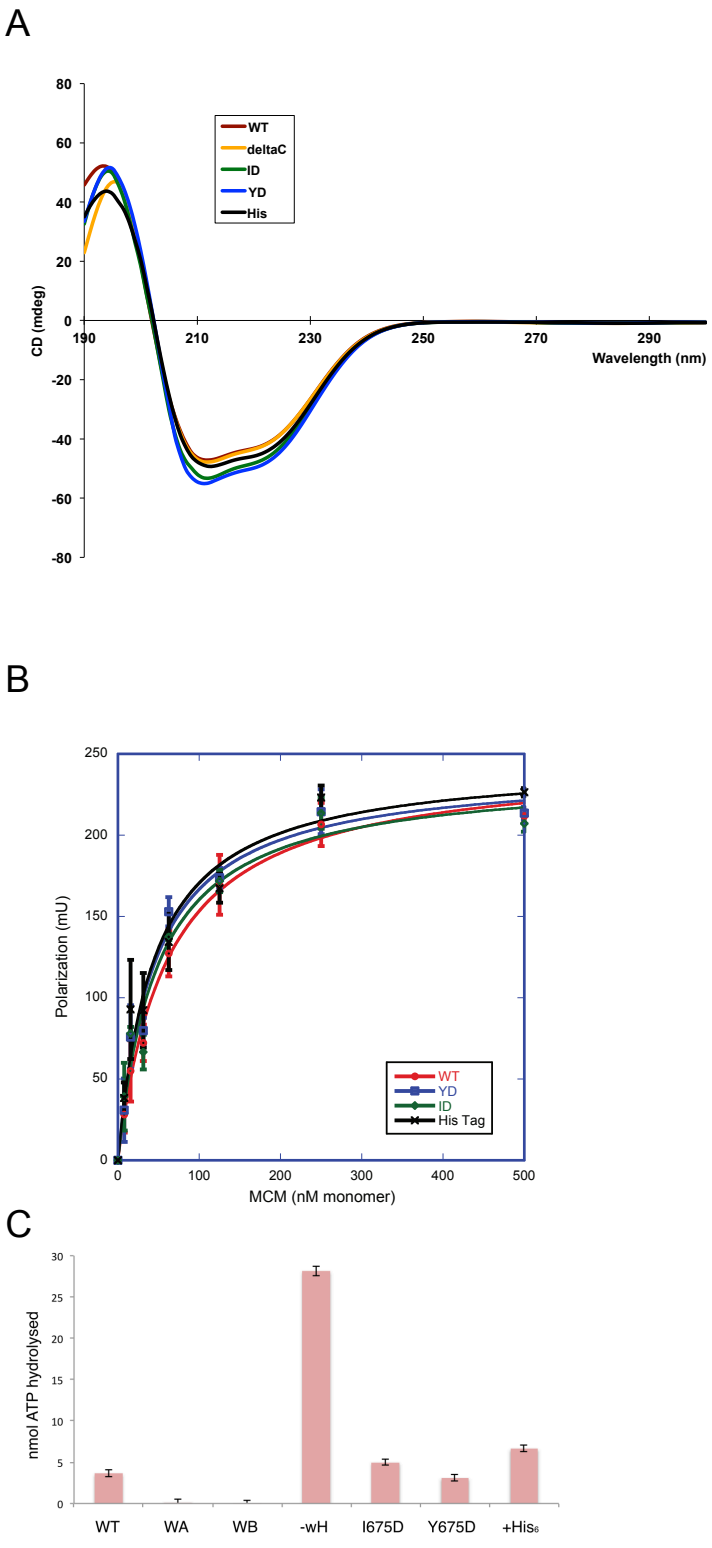

Figure S2. Related to Figure 3. Integrity and Activity of Mutant MCM Proteins. (A) Circular dichroism measurements of the indicated proteins. (B) Fluorescence polarization measurements of the indicated MCM proteins [wild-type (WT), I675D (ID), Y676D (YD) or C-terminally hexahistidine-tagged (His-tag)] binding to single-stranded DNA corresponding to the ORB2 site;

error bars are +/- the standard deviation. Measurements were performed in triplicate and fit to a single-site binding model using Kaleidagraph (version 4.5, Synergy Software). (C) ATPase assays confirm previous studies that Walker A (WA) and Walker B (WB) mutant MCMs lack ATPase activity and deletion of the wH domain (-WH) elevates the ATPase activity of MCM (Jenkinson and Chong, 2006; Moreau et al., 2007; Barry et al., 2007; Weidemann et al., 2015). In contrast, introduction of point mutations I675D or Y676D or addition of a C-terminal hexahistidine-tag results in ATPase activities similar to the wild-type protein (WT). Experiments were performed in triplicate and the error bars are +/- the standard deviation of the results.

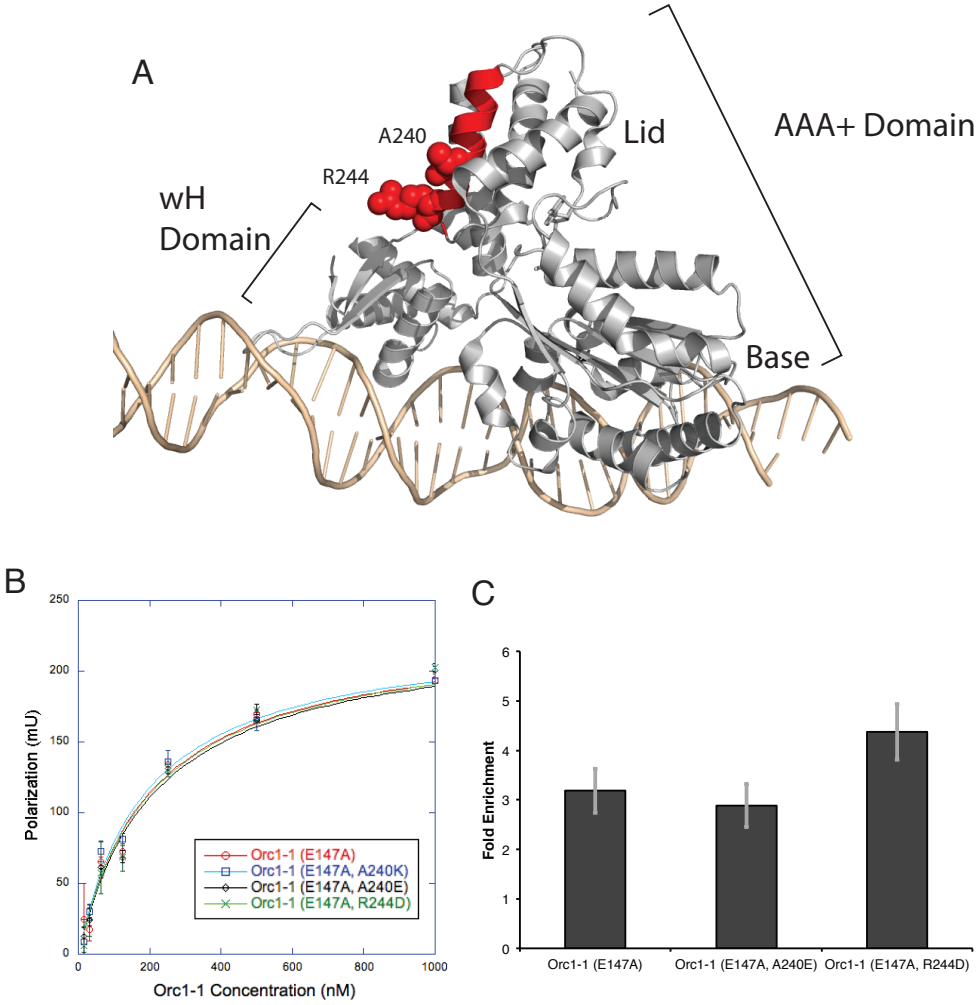

Figure S3. Related to Figure 4. Position of the MCM-Interaction Site on Orc1/Cdc6 Proteins. (A) Structure of Orc1-1•ADP on DNA. The alpha helix highlighted in red corresponds to the MCM recruitment helix, highlighted in Figure 4. The figure was generated using Pymol (Schrödinger, LLC) from PDB file 2QBY. (B) Fluorescence polarization measurements of the indicated Orc1-1 proteins binding to the ORB2 site, error bars are +/- the standard deviation. Measurements were performed in triplicate and fit to a single-site binding model using Kaleidagraph (version 4.5, Synergy Software). (C) ChIP experiments were performed with the indicated mutant proteins expressed in *S. islandicus* REY15A. Binding is expressed as fold-enrichment of Orc1-1 at *oriC1* over a control locus, as detailed in (Samson et al., 2013).

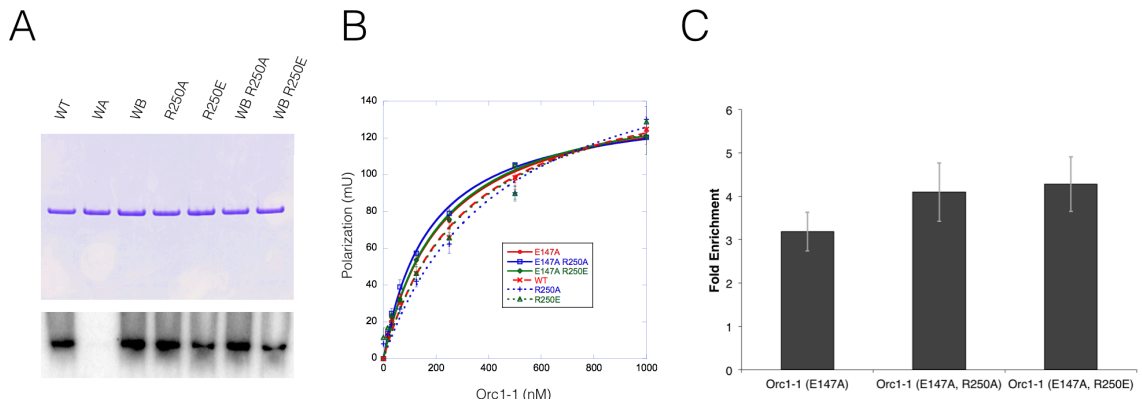

Figure S4. Related to Figure 5. ATP- and DNA-Binding Activities of Mutant Orc1-1 Proteins. (A) ATP binding by the indicated wild-type or mutant Orc1-1 proteins [WT = wild-type, WA = Walker A (K69A), WB = Walker B (E147A)]. 10 µg of the protein were incubated with 10 µCi of α-^{32}P ATP (3000 Ci/mmol). Reactions were split in two and half was subjected to SDS PAGE (upper panel). The other half was analyzed by native gel electrophoresis in Tris-glycine, before phosphorimager analysis of the wet gel (lower panel). (B) Fluorescence polarization measurements of the indicated Orc1-1 proteins binding to the ORB2 site, error bars are +/- the standard deviation. Measurements were performed in triplicate and fit to a single-site binding model using Kaleidagraph (version 4.5, Synergy Software). (C) ChIP experiments were performed with the indicated mutant proteins expressed in *S. islandicus* REY15A. Binding is expressed as fold-enrichment of Orc1-1 at *oriC1* over a control locus as detailed in (Samson et al., 2013).

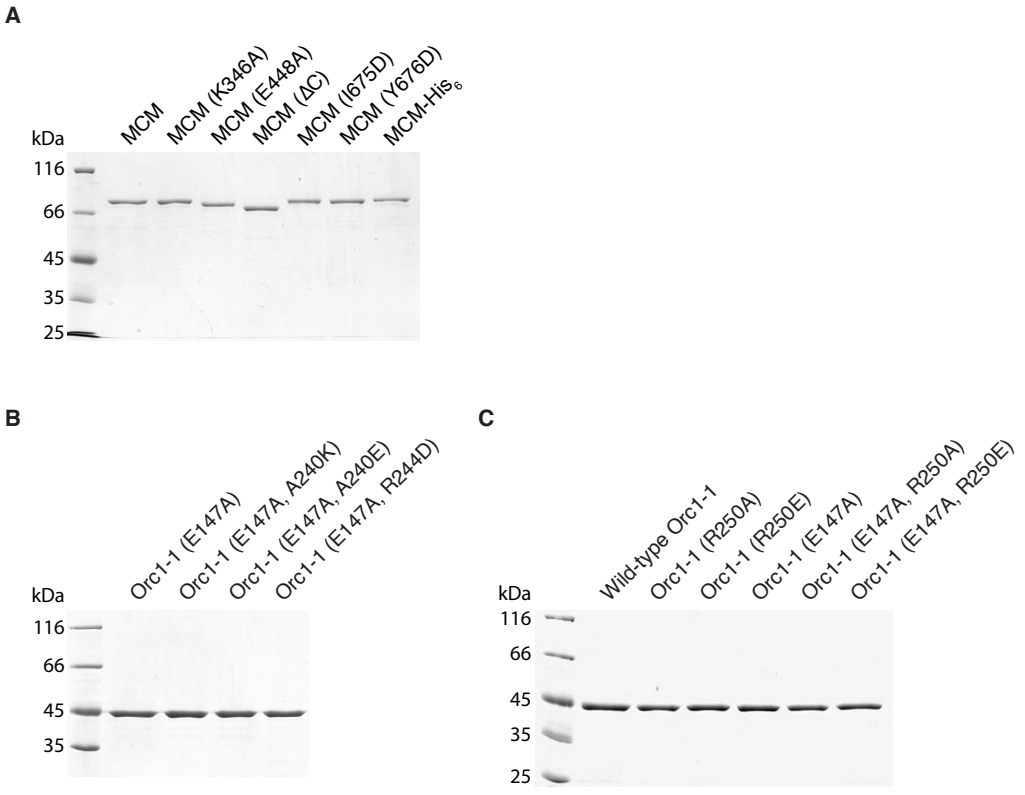

Figure S5. Related to Figures 1-6. Purified Recombinant Proteins Visualized by Coomassie Brilliant Blue Staining Following SDS-PAGE. (**A**) Wild-type and mutant MCM preparations (1 µg per lane). (**B**) Walker B and Walker B/MRM mutant Orc1-1 proteins (2 µg per lane). (**C**) Purified Orc1-1 Sensor 2 mutant proteins (2 µg per lane).

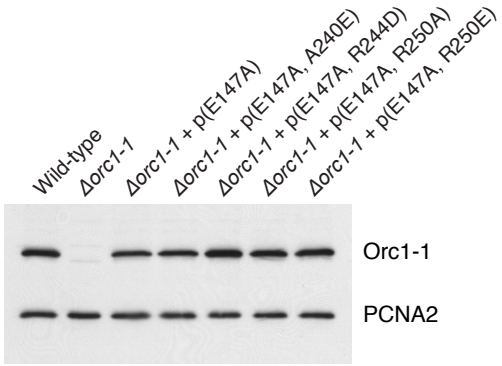

Figure S6. Related to Figures 4 and 5. Western Blot Analyses of Ectopic Orc1-1 Expression. Western blot analysis of Orc1-1 expression levels in wild-type, Δ*orc1-1* mutant and transformed Δ*orc1-1* mutant strains. The mutant form of the Orc1-1 protein being expressed from the pSSREF plasmid in the transformed strains is designated as p(X). PCNA2 protein levels were detected as a loading control for the western blot.

Genome Sequence ORF Reference	Uniprot Accession Number
Igni_1295	A8AC19
DKAM_1427	B8D6M2
SiRe_1231	F0NF18
SSO0771	Q9UXF8
Msed_2046	A4YID4
Ahos_0521	F4B6J9
SacRon12I_04365	M1IXE7
MTH1599	O27636
SacRon12I_00005	M1IUJ0
Msed_0701	A4YEM4
Ahos_0001	F4BA86
SiRe_0002	FONFE6
SSO2184	Q97WM8
MTH1412	O27463
CENSYa_1839	A0RYN2
DKAM_1377	B8D6H2
Igni_0250	A8A932
PAB2265	A8A932
SSO0257	Q980N4
SacRon12I_03475	M1IAX7
Ahos_0780	F4B7Y9
Msed_0001	A4YCM6
SiRe_1740	F0NBP2

Table S1 Genome sequence references for the open reading frames listed in Figure 4A with their corresponding Uniprot accession numbers. Related to Figure 4.

Supplemental Experimental Procedures

Identification of the relationship between the winged helix domains of MCM and RPA32

The initial identification of the relationship between these proteins arose from application of the Phyre2 structure prediction algorithm (Kelly et al, 2015). This program uses a hidden Markov modeling approach to generate 3D models of a candidate sequence.

Using *Sulfolobus islandicus* MCM residues 620-686 as a query, Phyre2 returned results with greater than 90% confidence as below.

Description	Confidence	% identity	PDB
S. solfataricus MCM	99.9	100	2M45
M. thermautotrophicus MCM	99.8	21	2MA3
Human RPA32 CTD	94.5	16	1DPU
Iron-dependent repressor	93.8	11	2ISY
MntR	93.7	21	2H09
IclR	92.8	23	1MKM
IdeR	92.8	12	2IT0
DtxR	91.4	12	1G3W
SSO2273	91	21	2X4H

The proteins highlighted in gray are a family of prokaryotic metal-dependent transcriptional regulators that possess winged-helix domains. SSO2273 is a protein of unknown function from *Sulfolobus solfataricus* that is predicted to be an iron-regulated transcriptional regulator.

Subsequently, a DALI search (Holm and Rosenstrom, 2010) with the structure of *S. solfataricus* MCM gave the following top ten hits in addition to *S. solfataricus* MCM itself. Z scores below 2 are spurious.

Description	Z	rmsd	lali	nres	%id	PDB
S. solfataricus MCM	15.7	0.0	67	87	100	2M45
M. thermautotrophicus MCM	10.5	1.2	64	88	20	2MA3
CST COMPLEX SUBUNIT STN1	10.1	2.2	66	168	15	4JQF
REPLICATION PROTEIN A 32 KDA SUBUNIT	10.0	1.6	62	65	15	4MQV
IRON-DEPENDENT TRANSCRIPTION REPRESSOR	9.9	1.5	60	213	12	4O6J
REPLICATION PROTEIN A 32 KDA SUBUNIT	9.8	1.5	61	65	15	4MQV
REPLICATION PROTEIN A 32 KDA SUBUNIT	9.7	1.6	62	66	15	4OU0
PUTATIVE METAL UPTAKE REGULATION PROTEIN	9.6	2.0	64	127	8	3MWM
REPLICATION PROTEIN A 32 KDA CTD	9.6	2.3	64	69	14	1DPU
HYPOTHETICAL PROTEIN SSO2273	9.5	1.7	61	129	16	2X4H
Fe DEP REGULATOR IdeR	9.4	1.5	60	213	12	4O5V

STN1 is a component of the Ten1/Stn1/Cdc13 complex that acts as a telomere-dedicated single-stranded DNA binding complex and is believed to be a paralog of the RPA heterotrimer. While RPA32 has a single C-terminal wH domain, Stn1 possesses two tandemly repeated C-terminal wH domains. As with their paralog in RPA, the wH domains act as a protein-protein interaction module (Lue et al, 2014)

The sequence alignment below reveals that the highlighted Ile and Tyr show a restricted conservation in these closest structural homologs of SsoMCM's wH domain.

```
                                                                **
SsoMCM     -KSAREKMMKIIEIIDSLAVSSECAKVKDILKEAQQVGIEKSNIEKLLTDMRKSGIIYEAKPECYKKV
MthMCM     ----RDKFRLLEEIKEYEDDYGRAPTNILITEMMDYNLSEEKVEELIRILKDKGAIFEPARGYLKIV
RPA32      LTVAQNQVMNFIKA----CPRPEGLNFQDLKNQLK--HLSVSSIKQAVDFLSNEGHIYSTDDDHLKST
Stn1       --EDKDLHRKIHRIIQQDCQKEKGCHFLHILACARLSISLSEAVLQQWLELLEDQSDIVSTMEHYYTAF
FeReg      --VTEEDYLKIIQELVLY---KGYATLADISESL---NLKRQSVRDELNHLISLSMAEKIERGKYFLT
SSO2273    --LSRREFSYLLTLI-KRYNDSGEGAKLNRIAKDL---KIAPSSVFEEVSHLEEKGLVKKKEDGVWIT
```

This is further emphasized by the structural comparison below. Here, as in Figure 3, residues that are identical between RPA32 and MCM are shown in yellow. If those residues are also identical in IdeR or SSO2273 they are colored yellow in the respective structure. The lower row shows a model generated by alignment and superposition of the various wH domains with that of RPA32. In addition to the lack of conservation of the interaction-surface residues, IdeR and SSO2273 show clear steric clashes with the modeled position of the UNG2 peptide.

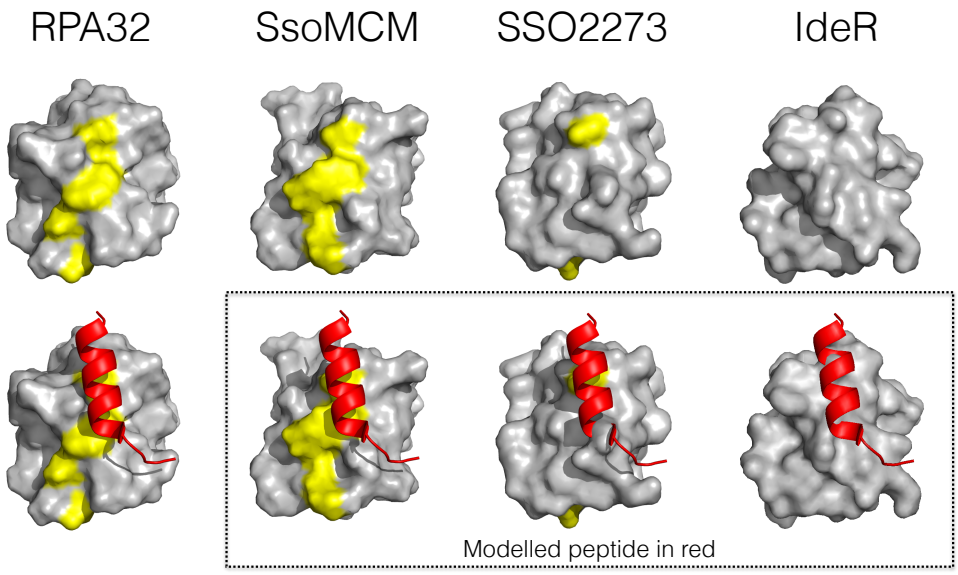

Supplementary References

Lue, N.F., Chan, J., Wright, W.E. and Hurwitz, J. (2014), The CDC13-STN1-TEN1 complex stimulates Pol α activity by promoting RNA priming and primase-to-polymerase switch. Nat. Comm. *5*. 5762